The Astrophysical Journal, 584:L99–L102, 2003 February 20

DOUBLY HELICAL CORONAL EJECTIONS FROM DYNAMOS AND THEIR ROLE IN SUSTAINING THE SOLAR CYCLE

Eric G. Blackman[1] and Axel Brandenburg[2]
Received 2002 December 1; accepted 2003 January 9; published 2003 January 20

ABSTRACT

Two questions about the solar magnetic field might be answered together once their connection is identified. The first is important for large-scale dynamo theory: what prevents the magnetic back-reaction forces from shutting down the dynamo cycle? The second question is, what determines the handedness of twist and writhe in magnetized coronal ejecta? Magnetic helicity conservation is important for answering both questions. Conservation implies that dynamo generation of large-scale writhed structures is accompanied by the oppositely signed twist along these structures. The latter is associated with the back-reaction force. We suggest that coronal mass ejections simultaneously liberate small-scale twist and large-scale writhe of opposite sign, helping to prevent the cycle from quenching and enabling a net magnetic flux change in each hemisphere. Solar observations and helicity spectrum measurements from our simulation of a rising flux tube support this idea. We show a new pictorial of dynamo flux generation that includes the back-reaction and magnetic helicity conservation and represents the field by a ribbon or tube rather than a line.

Subject headings: magnetic fields — MHD — stars: magnetic fields — Sun: coronal mass ejections (CMEs) — Sun: magnetic fields — turbulence

1. INTRODUCTION

The helical magnetic dynamo is the basis for a promising class of mechanisms to explain large-scale magnetic fields observed in stars and galaxies (Parker 1955, 1993; Moffatt 1978; Krause & Rädler 1980). The basic "α-Ω" dynamo is the specific version most relevant for strongly sheared rotators (Fig. 1). Interface α-Ω dynamos (Parker 1993; Charbonneau & MacGregor 1996; Markiel & Thomas 1999) include the fact that, unlike for galaxies and disks, the dominant shear layer is beneath the dominant turbulent region.

Focusing on the simplest "α-Ω" picture (Fig. 1), consider an initially weak toroidal (= encircling the rotation axis) loop of the magnetic field embedded in the astrophysical plasma rotator. The magnetic field is coupled to the plasma so the field is stretched in response the plasma motion. Now imagine, as in the Sun, that there is an outwardly decreasing density gradient. Conservation of angular momentum dictates that a rising swirl of gas threaded by a toroidal magnetic field will writhe oppositely to the underlying system's rotation. The swirl then gains a poloidal field component. Statistically, rising swirls in the northern (southern) hemisphere writhe the field clockwise (counterclockwise). This is the "α"-effect and is shown by the writhed loop of Figure 1*a* for the northern hemisphere. Differential rotation at the base of the loop shears the radial field (the "Ω"-effect). The bottom part of the loop amplifies the initial toroidal seed loop as shown in Figure 1*b*, whilst the top part of the loop diffused away (the "β"-effect). In doing so, magnetic flux is amplified; the flux penetrating the tilted rectangular surface is zero in Figure 1*a* but finite in Figure 1*b*.

This process is represented mathematically by averaging the magnetic induction equation over a local volume and breaking all quantities (velocity $\boldsymbol{U}$, magnetic field $\boldsymbol{B}$ in Alfvén velocity units, and normalized current density $\boldsymbol{J} \equiv \boldsymbol{\nabla} \times \boldsymbol{B}$) into their mean (indicated by an overbar) and fluctuating (indicated by lowercase) components. The result is Moffatt 1978, $\partial_t \overline{\boldsymbol{B}} = \boldsymbol{\nabla} \times (\alpha \overline{\boldsymbol{B}} + \overline{\boldsymbol{U}} \times \overline{\boldsymbol{B}}) + (\beta + \lambda)\nabla^2 \overline{\boldsymbol{B}}$, where λ is the microphysical diffusivity. The $\overline{\boldsymbol{U}}$ term incorporates the Ω-effect, the β term incorporates the turbulent diffusion (assuming constant β), and the first term on the right incorporates the α-effect. In the kinematic theory (Moffatt 1978), α is given by $\alpha = \alpha_0 = -(\tau/3)\overline{\boldsymbol{u} \cdot \boldsymbol{\nabla} \times \boldsymbol{u}}$. Here, τ is a turbulent damping time and $\boldsymbol{u} \cdot \boldsymbol{\nabla} \times \boldsymbol{u}$ is the kinetic helicity, which dictates the α-effect described above. Usually, α and β are prescribed as input parameters.

A long-standing problem has been the absence of properly incorporating the (time-dependent) back-reaction from the growing magnetic field on the turbulent motions. This stimulated criticisms of mean field dynamos (Piddington 1981; Cattaneo & Hughes 1996) and motivated interface dynamo models (Parker 1993). But the back-reaction is now better understood. Steady-state studies of α-quenching (Cattaneo & Hughes 1996) apply only at fully saturated dynamo regimes, not at early times, when the back-reaction is just beginning to be important. There the growth is fast and most relevant for astrophysics. Demonstrating this requires including the time evolution of the turbulent velocity, subject to magnetic forces. Carrying this out formally (Blackman & Field 2002) and using a closure in which triple correlations act as a damping term amounts to replacing $\alpha = \alpha_0$ with $\alpha = \alpha_0 + (\tau/3)\overline{\boldsymbol{j} \cdot \boldsymbol{b}}$, where the second term is the back-reaction. It arises from $\boldsymbol{j} \times \overline{\boldsymbol{B}}$, the force associated with the action of the small-scale current and the large-scale field. This residual form of α has been long thought (Pouquet, Frisch, & Leorat 1976) to be the real driver of the helical dynamo and has been employed in attempts to understand its quenching (Zeldovich, Ruzmaikin, & Sokoloff 1983; Kleeorin & Ruzmaikin 1982; Field & Blackman 2002; Blackman & Brandenburg 2002; Bhattacharjee & Yuan 1995; Blackman & Field 2002; Gruzinov & Diamond 1995). A large $\overline{\boldsymbol{j} \cdot \boldsymbol{b}}$ can quench the dynamo.

In § 2, we summarize the successful back-reaction theory and show how it predicts ejection of twist and writhe of opposite sign. In § 3, we give a new pictorial of dynamo action that includes magnetic helicity conservation and discuss a sim-

[1] Department of Physics and Astronomy and Laboratory for Laser Energetics, University of Rochester, Rochester, NY 14627.
[2] Nordita, Blegdamsvej 17, DK-2100 Copenhagen Ø, Denmark.

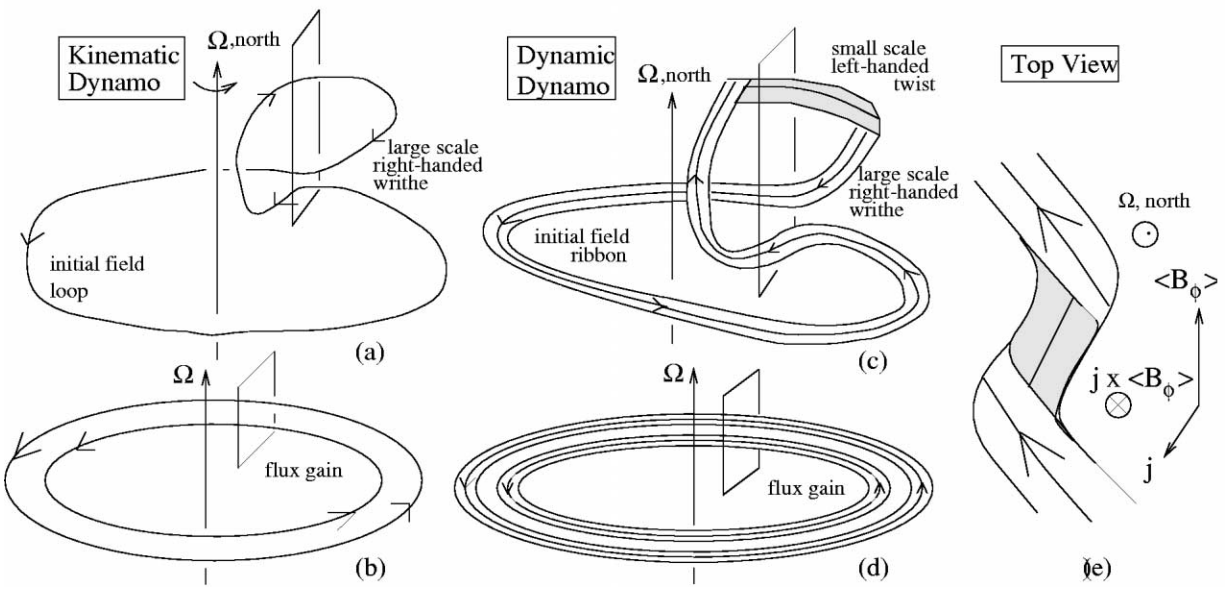

FIG. 1.—Schematic of *kinematic* helical α-Ω dynamo in northern hemisphere is shown in (*a*) and (*b*), while the *dynamic* helical α-Ω dynamo is shown by analogy in (*c*) and (*d*). The mean field is represented as a line in (*a*) and (*b*) and as a tube in (*c*) and (*d*). (*a*) From an initial toroidal loop, the α-effect induces a rising loop of right-handed writhe that gives a radial field component. (*b*) Differential rotation at the base of the loop shears the radial component, amplifying the toroidal component, and the ejection of the top part of loop (through CMEs) allows for a net flux gain through the rectangle. (*c*) Same as (*a*) but with the field represented as a flux tube. This shows how the right-handed writhe of the large-scale loop is accompanied by a left-handed twist along the tube, incorporating magnetic helicity conservation. (*d*) Same as (*b*) but with field represented as a ribbon/tube. (*e*) Top view of the combined twist and writhe that can be compared with observed coronal magnetic structures in active regions. Note the N shape of the right-handed large-scale twist in combination with the left-handed small-scale twist along the tube. The back-reaction force that resists bending is seen to result from the small-scale twist. Diffusing the top part of the loops allows for net flux generation in the rectangles of (*a*)–(*d*) and alleviates the back-reaction that could otherwise quench the dynamo.

ulation of a rising flux tube. Observational implications are discussed in § 4, and we conclude in § 5.

2. ROLE OF MAGNETIC HELICITY CONSERVATION

The principle of magnetic helicity conservation determines the strength of the current helicity correction term in α discussed in the previous section. The magnetic helicity, defined by a volume integral $H \equiv \int \boldsymbol{A}\cdot\boldsymbol{B}\, dV \equiv \langle \boldsymbol{A}\cdot\boldsymbol{B}\rangle V$, satisfies (Woltjer 1958; Berger & Field 1984)

$$\partial_t H = -2\lambda C - \text{surface terms}, \tag{1}$$

where the magnetic field $\boldsymbol{B}$ is related to $\boldsymbol{A}$ by $\boldsymbol{B} = \boldsymbol{\nabla}\times\boldsymbol{A}$ and the current helicity C is defined by $C \equiv \langle \boldsymbol{J}\cdot\boldsymbol{B}\rangle V$. Without the surface terms (which represent flow through boundaries), H is well conserved: for $\lambda \to 0$, the λ term in equation (1) converges to zero (Berger 1984).

The magnetic helicity is a measure of "linkage" and "twist" of field lines (Berger & Field 1984). Equation (1) then means that in a closed system, the total amount of twist and writhe is conserved. If the large-scale field is writhed one way, then the small-scale field must twist oppositely. In the Sun, differential rotation and cyclonic convection (the α-effect) are both sources of helicity (Berger & Ruzmaikin 2000; DeVore 2000), but here we focus on the α-effect, which generates large-scale poloidal structures.

The α-effect does not produce a net magnetic twist but produces simultaneously positive and negative magnetic twists on different scales (Seehafer 1996; Ji 1999; Blackman & Field 2000; Brandenburg 2001; Field & Blackman 2002). The importance of this scale segregation of H for the back-reaction term in α is easily seen in the two-scale approach. Here we write $H = H_1 + H_2$, where $H_1 = \langle \boldsymbol{A}\cdot\overline{\boldsymbol{B}}\rangle V$ and $H_2 = \langle \boldsymbol{a}\cdot\boldsymbol{b}\rangle V$ correspond to the volume-integrated large- and small-scale contributions, respectively. For C, we then have $C = \langle \overline{\boldsymbol{J}}\cdot\overline{\boldsymbol{B}}\rangle V + \langle \boldsymbol{j}\cdot\boldsymbol{b}\rangle V = k_1^2\boldsymbol{H}_1 + k_2^2\boldsymbol{H}_2$, where k_1 and k_2 represent the wavenumbers (inverse gradients) associated with the large and small scales, respectively, and the second equality follows rigorously for a closed system. The current helicity back-reaction in $\langle\alpha\rangle$ is thus $k_2^2 H_2$.

We now relate $\overline{\boldsymbol{B}}$ to $\underline{H}_1$. We define ϵ_1 such that the large-scale magnetic energy $\langle \overline{\boldsymbol{B}}^2\rangle V = H_1 k_1/\epsilon_1$ and where $0 < |\epsilon_1| \le 1$, where $|\epsilon_1| = 1$ only for a force-free helical large-scale field (i.e., for which $\overline{\boldsymbol{J}} \| \overline{\boldsymbol{B}}$, so that the force $\overline{\boldsymbol{J}}\times\overline{\boldsymbol{B}} = 0$). In the northern hemisphere $\epsilon_1 > 0$. By writing conservation equations analogous to equation (1) for H_1 and H_2, respectively, we obtain

$$\partial_t H_1 = 2S - 2\lambda k_1^2 H_1 - \text{surface terms}, \tag{2}$$

$$\partial_t H_2 = -2S - 2\lambda k_2^2 H_2 - \text{surface terms}, \tag{3}$$

where we have used $S = (\langle\alpha\rangle k_1/\epsilon_1 - \langle\beta\rangle k_1^2)H_1$ and $\langle\alpha\rangle = [\langle\alpha_0\rangle + (1/3)\,\tau k_2^2 H_2/V]$. The case without surface terms and with $\epsilon_1 = 1$ represents a dynamo without differential rotation. The solution (Field & Blackman 2002; Blackman & Brandenburg 2002; Blackman & Field 2002) shows that for initially small H_2 but large α_0, H_1 grows. Growth of H_1 implies the oppositely signed growth of H_2. This H_2 back-reacts on α_0, ultimately quenching $\langle\alpha\rangle$ and the dynamo.

Since the Sun is a differentially rotating open system, shear and surface terms are important. The former forces $|\epsilon_1| < 1$ and ϵ_1 a function of time to reflect the solar cycle. The presence of surface terms generally requires use of the relative magnetic helicity (Berger & Field 1984), but to capture the key points, we instead treat them as diffusion terms (Brandenburg, Dobler, & Subramanian 2002). We combine the λ and surface terms

of both equations (2) and (3) into the forms $-\nu_1 k_1^2 H_1$ and $-\nu_2 k_2^2 H_2$, respectively. The volume average, $\langle\,\rangle$, is taken over one hemisphere, and surface terms represent diffusion into the corona. On timescales much shorter than the 11 yr solar half-cycle, the left sides of equations (2) and (3) are negligible and the system is in a relatively steady state. We then see that the boundary terms are equal and opposite (Blackman & Field 2000). Here this implies $\nu_1 k_1^2 |H_1| \simeq \nu_2 k_2^2 |H_2|$. Since the boundary diffusion terms represent a flux of (relative) magnetic helicity to the exterior, these quantities are connected to measurable observables. We therefore predict that the shedding rates of small-scale twist and large-scale writhe from the α-effect are equal in magnitude and opposite in sign.

3. REVISING THE "TEXTBOOK" DYNAMO PICTORIAL

The helicity conservation, shedding, and magnetic back-reaction are represented in Figures 1*c*–1*e* for the northern hemisphere. Comparing Figures 1*a* and 1*b* (*H* conservation not included) with Figures 1*c* and 1*d* (*H* conservation included), we see that in the latter, as the α-effect produces its large-scale writhe (the loop corresponding to gradient scale k_1^{-1}), it also twists the tube (corresponding to gradient scale k_2^{-1}). The large-scale writhe is right-handed, but the twist along the tube is left-handed, thus conserving total *H*.

The tube should be thought of as a mean field, averaged over smaller fluctuations. The top view is shown in Figure 1*e* for comparison to observations. In the northern hemisphere, we expect an N-shaped sigmoid prominence, and in the southern hemisphere we would expect an S-shaped sigmoid. In Figure 1*e*, we also show the back-reaction force corresponding to the small-scale magnetic twist along the tube: it fights against writhing or bending. Eventually, this twisting would suppress the α-effect (and thus statistically, its hemispheric average $\langle\alpha\rangle$ entering eqs. [2] and [3]), which thrives on being able to writhe the tube. In the Sun, such sigmoid structures precede coronal mass ejections (CMEs; Pevtsov & Canfield 1999), which dissipate both the writhe and the twist on timescales of the order of days or weeks. In doing so, they help alleviate the back-reaction on the α-effect and allow a net amplification of magnetic flux, as shown in Figure 1*c*. Some loops produced by the dynamo may not escape, implying that some of the simultaneous diffusion of H_1 and H_2 is hidden in the solar interior. Even so, the helicity fluxes of H_1 and H_2 from the loops that do escape can be equal and opposite. Getting rid of H_2 simultaneously with H_1 alleviates the back-reaction, and external removal by CMEs is one mechanism to do so. Removal of H_2 allows the α-effect to be again driven by α_0 at solar minimum, allowing the cycle to repeat.

We have performed a numerical simulation to measure the magnetic helicity spectrum of a buoyant magnetic flux tube in the presence of rotation. This confirms the basic idea that twist and writhe emerge with opposite sign. Previous simulations of rising tubes (Abbett, Fisher, & Fan 2000) did not focus on the magnetic helicity spectrum. We started with a toroidal horizontal flux tube and a vertically dependent sinusoidal modulation of the entropy along the tube. This destabilizes the tube to buckle and rise in one portion. The boundaries were sufficiently far away to use a Fourier transform to obtain power spectra (Fig. 2). After six free-fall times, the spectrum shows mostly positive magnetic helicity together with a gradually increasing higher wavenumber component of negative spectral helicity density. The latter is the anticipated contribution from the twist along the tube.

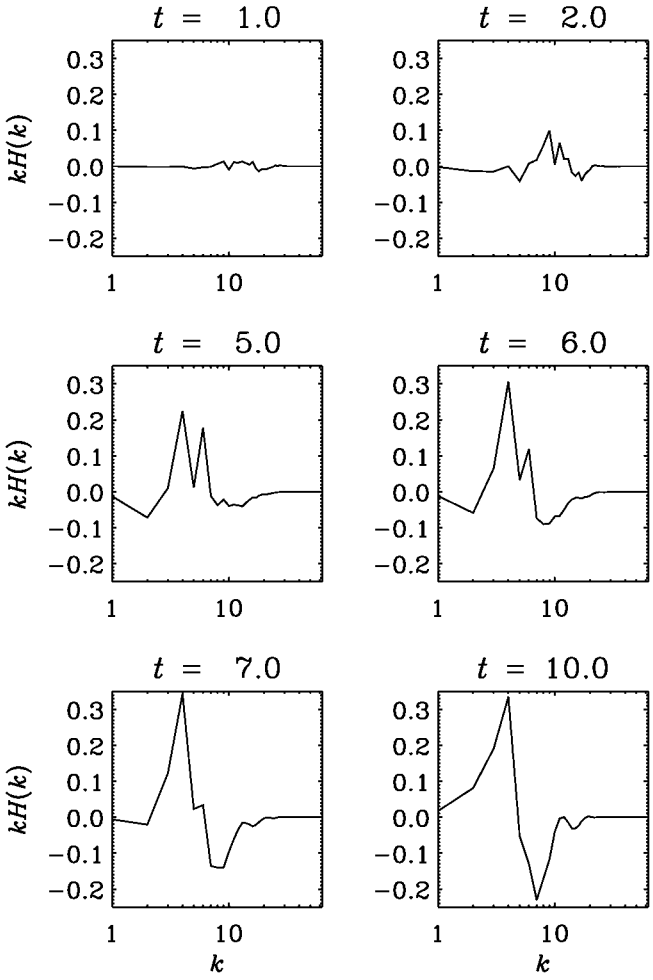

FIG. 2.—Magnetic helicity spectra from rising flux tube simulation (scaled by wavenumber *k* to give magnetic helicity per logarithmic interval) taken over the entire computational box. Positive (negative) helicity dominates at small (large) wavenumber.

4. IMPLICATIONS AND COMPARISONS TO OBSERVATIONS

Note that the magnetic helicity is a volume integral, so the tube on which the twisted prominence arises may have a hidden twist elsewhere inside the Sun. This subtlety can be accounted for by use of the relative magnetic helicity (Berger & Field 1984), which allows a quantifiable interpretation of locally twisted structures. Observations typically measure the current helicity density, $\boldsymbol{J}\cdot\boldsymbol{B}$, within a single structure, from which hemispheric averages can be computed or the surface-integrated relative magnetic helicity fluxes.

Existing observations are consistent with our basic ideas. First, the observed N sigmoids outnumber S sigmoids by a ratio of 6 : 1 in the northern hemisphere, with the expected reverse relation in the southern hemisphere (Rust & Kumar 1996). Second, sigmoid studies (Gibson et al. 2002 and references therein) also show qualitative agreement with our picture: Figure 2*a* of Gibson et al. (2002) shows a *Transition Region and Coronal Explorer* image of an N sigmoid (right-handed writhe) with left-handed twisted filament of the active region NOAA Active Region 8668, typical of the northern hemisphere just as we predict. (Our theory is statistical, so the occasional N sigmoid such as AR 8100 [Green et al. 2002] in the southern hemisphere is not alarming. But even for AR 8100, the writhe is opposite in sign to the twist along the prominence.)

Other studies also confirm a basic hemispheric dependence of the sign of small-scale current helicity, corresponding to the twist along the tube in Figure 1*c*. Measurements of current helicity densities, surface-integrated relative magnetic helicity fluxes (Chae 2000; Berger & Ruzmaikin 2000), and fits to line-of-sight magnetograms of solar active regions (Seehafer 1990; Rust & Kumar 1996; Bao et al. 1999; Pevtsov & Latushko 2000) show primarily negative values in the north and positive in the south. These studies measure the sign of the small-scale twist along the tube (Rädler & Seehafer 1990). The twist is expected at the apex of a writhed prominence; there the density is lowest (Parker 1974; Choudhuri 2002).

In sum, Figure 1*e*, showing an N sigmoid, is consistent with the dominant structures of the northern hemisphere. Large-scale positive writhe dominates in the north, and large-scale negative writhe dominates in the south. Small-scale twists along the prominences are predominantly negative in the north and positive in the south, so as to produce a very small net helicity in each hemisphere. This is complementary to Démoulin et. al (2002), in which oppositely signed twist and writhe from shear were shown to be able to largely cancel, producing a small total magnetic helicity. Here we focused on the α-effect that has the same effect. Finally, note that our $\overline{\boldsymbol{B}}$ represents a local averaging over the small-scale twist so that $\overline{\boldsymbol{B}}$ has only the writhe (Fig. 1*a* is thus applicable to $\overline{\boldsymbol{B}}$, whereas Fig. 1*c* shows both $\overline{\boldsymbol{B}}$ and $\boldsymbol{b}$). On even larger scales, the globally averaged field computed by an azimuthal average $\langle \overline{\boldsymbol{B}}_{\phi} \rangle$ is weaker than $\overline{\boldsymbol{B}}_{\phi}$ in a local structure because of the small filling fraction.

5. CONCLUSION

A new understanding of how helical dynamos conserve magnetic helicity may help resolve several mysteries of the solar magnetic field. We have suggested that large- and small-scale helicities of approximately equal magnitude should be ejected into the solar corona as part of the sustenance of the solar cycle. The large-scale helicity corresponds to the writhe of a prominence, whilst the small-scale helicity corresponds to the twist along the prominence. We emphasize the importance of simultaneously detecting large- and small-scale contributions to the losses of helical magnetic fields in pre-CME sigmoid structures at the solar surface. Figure 1 illustrates our basic concepts through a new pictorial representation of the mean field dynamo that includes magnetic helicity conservation and the back-reaction.

Existing observations are roughly consistent with our basic idea, but more work is needed to test them and to incorporate them into global dynamo models that capture other features of the solar cycle. It is also possible that the cancellation of large- and small-scale helicities through the surface is not exact, so that the internal diffusion and boundary terms are scale dependent. The cancellation of large- and small-scale helicities would then occur through some combination of surface and internal diffusion. Determining such a scale dependence is important for further testing the ideas herein and generalizing them.

E. G. B. acknowledges DOE grant DE-FG02-00ER54600 and the Department of Astrophysical Sciences at Princeton for hospitality. The Particle Physics and Astronomy Research Council–supported supercomputers at Leicester and St. Andrews and the Odense Beowulf cluster are acknowledged.

REFERENCES

Abbett, W. P., Fisher, G. H., & Fan, Y. 2000, ApJ, 540, 548
Bao, S. D., Zhang, H. Q., Ai, G. X., & Zhang, M. 1999, A&AS, 139, 311
Berger, M. A. 1984, Geophys. Astrophys. Fluid Dyn., 30, 79
Berger, M., & Field, G. B. 1984, J. Fluid Mech., 147, 133
Berger, M. A., & Ruzmaikin, A. 2000, J. Geophys. Res., 105, 10481
Bhattacharjee, A., & Yuan, Y. 1995, ApJ, 449, 739
Blackman, E. G., & Brandenburg, A. 2002, ApJ, 579, 359
Blackman, E. G., & Field, G. B. 2000, MNRAS, 318, 724
———. 2002, Phys. Rev. Lett., 89, 265007
Brandenburg, A. 2001, ApJ, 550, 824
Brandenburg, A., Dobler, W., & Subramanian, K. 2002, Astron. Nachr., 323, 99
Cattaneo, F., & Hughes, D. W. 1996, Phys. Rev. E, 54, 4532
Chae, J. 2000, ApJ, 540, L115
Charbonneau, P., & MacGregor, K. B. 1996, ApJ, 473, L59
Choudhuri, A. R. 2002, preprint (astro-ph/0211591)
Démoulin, P., Mandrini, C. H., Van Driel-Gesztelyi, L., Lopez Fuentes, M. C., & Aulanier, G. 2002, Sol. Phys., 207, 87
DeVore, C. R. 2000, ApJ, 539, 944
Field, G. B., & Blackman, E. G. 2002, ApJ, 572, 685
Gibson, S. E., et al. 2002, ApJ, 574, 1021
Green, L. M., López Fuentes, M. C., Mandrini, C. H., Démoulin, P., Van Driel-Gesztelyi, L., & Culhane, J. L. 2002, Sol. Phys., 208, 43
Gruzinov, A. V., & Diamond, P. H. 1995, Phys. Plasmas, 2, 1941
Ji, H. 1999, Phys. Rev. Lett., 83, 3198
Kleeorin, N. I., & Ruzmaikin, A. A. 1982, Magnetohydrodynamics, 18, 116
Krause, F., & Rädler, K.-H. 1980, Mean-Field Magnetohydrodynamics and Dynamo Theory (Berlin: Akademie)
Markiel, J. A., & Thomas, J. H. 1999, ApJ, 523, 827
Moffatt, H. K. 1978, Magnetic Field Generation in Electrically Conducting Fluids (Cambridge: Cambridge Univ. Press)
Parker, E. N. 1955, ApJ, 122, 293
———. 1974, ApJ, 191, 245
———. 1993, ApJ, 408, 707
Pevtsov, A. A., & Canfield, R. C. 1999, Geophys. Monogr., 111, 103
Pevtsov, A. A., & Latushko, S. M. 2000, ApJ, 528, 999
Piddington, J. H. 1981, Cosmical Electrodynamics (Malbar: Krieger)
Pouquet, A., Frisch, U., & Leorat, J. 1976, J. Fluid Mech., 77, 321
Rädler, K.-H., & Seehafer, N. 1990 in Topological Fluid Mechanics, ed. H. K. Moffatt & A. Tsinober (Cambridge: Cambridge Univ. Press), 157
Rust, D. M., & Kumar, A. 1996, ApJ, 464, L199
Seehafer, N. 1990, Sol. Phys., 125, 219
———. 1996, Phys. Rev. E, 53, 1283
Woltjer, L. 1958, Proc. Natl. Acad. Sci., 44, 80
Zeldovich, Ya. B., Ruzmaikin, A. A., & Sokoloff, D. D. 1983, Magnetic Fields in Astrophysics (New York: Gordon & Breach)